

Amplitudes for $gg \rightarrow VV'$ and their high energy SUSY constraints.

G.J. Gounaris^a, J. Layssac^b, and F.M. Renard^b

^aDepartment of Theoretical Physics, Aristotle University of Thessaloniki,
Gr-54124, Thessaloniki, Greece.

^bLaboratoire de Physique Théorique et Astroparticules, UMR 5207
Université Montpellier II, F-34095 Montpellier Cedex 5.

Abstract

We study how the property of asymptotic helicity conservation (HCns), expected for any 2-to-2 process in the minimal supersymmetric model (MSSM), is realized in the processes $gg \rightarrow \gamma\gamma, \gamma Z, ZZ, W^+W^-$, at the 1loop electroweak order and very high energies. The violation of this property for the same process in the standard model (SM), is also shown. This strengthens the claim that HCns is specific to the renormalizable SUSY model, and not generally valid in SM. HCns strongly reduces the number of non-vanishing 2-to-2 amplitudes at asymptotic energies in MSSM.

PACS numbers: 12.15.-y, 12.15.-Lk, 14.70.Fm, 14.80.Ly

1 Introduction

Supersymmetry confers the remarkable Helicity Conservation (HCns) property to all the $2 \rightarrow 2$ amplitudes, at high energy and fixed angle. This was established to all perturbation orders in [1, 2], for the minimal supersymmetric model (MSSM); provided the energy is so high, that all SUSY masses can be neglected. Renormalizability is essential in proving HCns, since any known anomalous coupling would violate it [3].

More explicitly, HCns states that for any process

$$a_{\lambda_a} + b_{\lambda_b} \rightarrow c_{\lambda_c} + d_{\lambda_d} \quad , \quad (1)$$

with λ_j denoting the particle¹ helicity, all non-vanishing amplitudes at asymptotic energies and fixed angles, must be helicity conserving (HC), satisfying

$$\lambda_a + \lambda_b = \lambda_c + \lambda_d \quad . \quad (2)$$

Consequently, all helicity amplitudes that violate (2), must vanish at energies much larger than the SUSY scale, at fixed angles. Such amplitudes are termed as helicity violating (HV) ones. Evidently, HCns drastically reduces the number of the relevant asymptotic amplitudes in SUSY.

For processes involving external gauge bosons, the HCns theorem appears striking even at the Born level, where huge cancelations among the various diagrams contrive for its validity.

If the Born contribution to a process is non-vanishing, then HCns is approximately correct in the standard model (SM) also, up to the 1loop leading-log order [1, 2, 3, 4]. By this we mean that in such an SM case, the HV amplitudes, although not necessarily vanishing, are usually much smaller than the HC ones [5, 6, 7].

An approximate validity of HCns in SM, has also been observed at 1loop, in $\gamma\gamma \rightarrow \gamma\gamma$, γZ , ZZ , where the W -loop contribution is so overwhelming, that it renders the difference between SM and MSSM tiny [8, 9, 10, 11]. Thus the exact HCns validity in MSSM, forces its approximate validity in SM.

Since the HCns proof in [1, 2] was done by neglecting all SUSY soft breaking masses and the μ -term, the worry that terms involving ratios of masses might possibly invalidate the general proof in [1, 2], comes to mind. The only feasible way to address such worries, is through detail 1loop calculations, keeping all mass terms. The realization of helicity conservation as the energy increases, may then be investigated.

This was first investigated in detail 1loop electroweak (EW) calculations for $ug \rightarrow dW^+$ [4] and² $ug \rightarrow \tilde{d}_L \tilde{\chi}_j^+$ [12], which confirm HCns for these processes, and leads to interesting asymptotic SUSY relations among the corresponding unpolarized differential cross sections [4, 12]. These cross section relations turn out to be approximately correct even at LHC-like energies, for a wide range of SUSY benchmarks [13, 14, 15, 16, 17].

¹Scalar, fermion or gauge boson.

² $\tilde{\chi}_j^+$ describes a chargino.

Subsequently, the study of the gluon-fusion processes $gg \rightarrow HH'$, VH , to 1loop EW order, was done, where H , H' are Higgs or Goldstone bosons and $V = \gamma, Z, W^\pm$ [18]. The interest here is that there is neither a Born nor a W -loop contribution, like the one dominating the $\gamma\gamma$ processes mentioned above. So, there was a chance to find processes where HCns is strongly violated in SM, while of course always obeyed in MSSM [18]. Such properties were indeed found in $gg \rightarrow H_{SM}H_{SM}$ involving the SM Higgs particles; as well as in the Goldstone involving processes $gg \rightarrow G^0G^0$, G^+G^- , and $gg \rightarrow Z_LG^0$, $W_L^+G^-$, related through the equivalence theorem [19, 20, 21, 18].

The purpose of the present work is to explore the validity of HCns in MSSM, and its violation in SM, in the $gg \rightarrow VV'$ processes for $VV' = \gamma\gamma, \gamma Z, ZZ, W^+W^-$, calculated at the 1loop EW order. In this case, we should meet HC amplitudes involving transverse, as well as longitudinal, gauge bosons, and hopefully find many new instances, where HCns is realized in MSSM, and strongly violated in SM.

In achieving this, we construct simple analytic expressions for all the 1loop helicity amplitudes at asymptotic energies, in either SM or MSSM. At such high energies, the amplitudes only depend on the gauge couplings, and they either go to generally angle-dependent "constants", or vanish.

In MSSM, in agreement with HCns, only the HC amplitudes survive asymptotically; while the HV amplitudes go to zero, due to spectacular cancelations among the quark and squark contributions.

In SM though, all HV amplitudes with the final gauge bosons being either both transverse or both longitudinal, go asymptotically to constants, similar in magnitude to the HC amplitudes. Only those where one of the final gauge bosons is transverse and the other longitudinal, continue to vanish in SM.

Thus $gg \rightarrow VV'$ provide a rich set of examples where HCns is strongly violated in SM, while obeyed in MSSM. This further strengthens the claim that HCns is a genuine SUSY property [1, 2]. Such processes have been studied before, but the helicity properties of the amplitudes were not noticed [22].

A Fortran code supplying the complete 1loop helicity amplitudes for all the $gg \rightarrow VV'$ processes, in either SM or MSSM, at any c.m. energy and angle, is released in [23]. Using these, we present illustrations in SM and MSSM. The implied cross sections induced from the $gg \rightarrow \gamma\gamma, \gamma Z, ZZ, W^+W^-$ contributions at LHC, are also shown, in MSSM and SM. If the squarks lie in the TeV region, the MSSM changes to the $gg \rightarrow ZZ, W^+W^-$ cross sections, relative to the SM ones, are found at the (20-30)% level for TeV c.m. energies. We argue that such effects may be observable.

The contents of the paper are the following. Sect.2 summarizes the complete one loop calculation of $gg \rightarrow VV'$. In Sect.3 we present the simple analytic expressions for the high energy limit of the various amplitudes, in both MSSM and SM. In Sect.4, the Fortran code is introduced and various illustrations for the amplitudes and cross sections are given. A summary of the results and possible future developments are given in Sect.5.

2 The $gg \rightarrow VV'$ diagrams and amplitudes.

The gluon-fusion processes to two electroweak (EW) vector bosons addressed here are

$$g^a(l, \mu)g^b(l', \mu') \rightarrow V(p, \tau)V'(p', \tau') \quad , \quad (3)$$

where $(VV' = \gamma\gamma, \gamma Z, ZZ, W^+W^-)$. Here (l, l', p, p') describe the momenta of incoming gluons and outgoing vector bosons, while (μ, μ', τ, τ') denote their corresponding helicities. The indices a, b in (3) denote the gluon color, so that non-vanishing amplitudes could only appear for $a = b$.

Following the standard Jacob-Wick conventions [24], the helicity amplitudes for these processes are denoted as

$$F_{\mu\mu'\tau\tau'}^{VV'}(\sqrt{s}, \theta) \quad , \quad (4)$$

where (\sqrt{s}, θ) describe the subprocess c.m. energy and angle, while \sqrt{S} denotes the total LHC c.m. energy. A gluon color factor δ^{ab} is always removed from the F -amplitude, defined so that the phase of iF coincides with the S-matrix phase.

For the gluons we always have $(\mu, \mu' = \pm 1)$. Depending on the final vector-boson-helicities, the amplitudes where both VV' are transverse are referred to as transverse-transverse (TT), those where one is transverse and the other longitudinal are called LT or TL amplitudes, while those with $\tau = \tau' = 0$ are called LL amplitudes.

As already said, there is no Born EW contribution to the processes in (3). Non-vanishing contributions first arise at 1loop, where the needed independent graphs for MSSM are shown in Fig.1. A subset of these graphs involving only quark exchanges, and where Higgs exchange corresponds to H_{SM} , determines the SM result.

The squark-exchange bubbles C , C' , C'' and the triangle D in Fig.1 are by definition symmetric under the exchange of the two initial gluons. All others must be gg -symmetrized by adding the corresponding gluon symmetrization (gSYM) contribution though the interchange

$$\mu \leftrightarrow \mu' \quad , \quad \cos \theta \leftrightarrow -\cos \theta \quad , \quad \sin \theta \leftrightarrow -\sin \theta \quad . \quad (5)$$

Taking gSYM into account, we immediately see that charge conjugation forces the triangles A' and B' , and the bubble C' to vanish separately.

Since in the graphs of Fig.1, we never exchange V and V' , the antiquark or antisquark loop contributions are sometimes physically distinct and must be added. This is the case for the F -box. For the H -box though, the quark and antiquark loops have the same physical origin, and therefore only one must be considered. The calculation of the F and H boxes, was particularly laborious, since it needed traces of eight gamma matrices, with or without an additional³ γ_5 , leading to boxes with at most two different masses along the internal lines.

³Only needed for the W^+W^- amplitudes.

Correspondingly, the squark and antisquark loops provide physically distinct contributions, to the triangles D , E , E' and the box G , and should both be included. On the contrary, for the box J , only the squark loop must be taken into account, since the antisquark loop describes the same effect.

Adding all non-vanishing graphs in Fig.1 and performing the appropriate gSYM, all divergences cancel out. This is realized as follows. Triangle A and the sum of the graphs $B + C$ are convergent. Quark boxes F, H are divergent, but $F + H$ is convergent. Squark graphs C'', D' are divergent, but $C'' + D'$ is convergent. Squark triangles D, E, E' and the bubble C''' are divergent, but the divergence of their sum cancels against the divergence of the boxes $G + J$.

The calculation of the graphs in Fig.1 was done analytically, expressing the helicity amplitudes defined in (4), in terms of Passarino-Veltman functions [25], multiplied by forms depending on the particle-helicities and the c.m. energy and angle.. For simplicity, we have neglected CP violation in either SM or MSSM. The amplitudes satisfy the following symmetries [24]:

Bose-statistics for the initial gluons gives

$$F_{\mu\mu'\tau\tau'}^{VV'}(\theta) = (-1)^{\tau-\tau'} F_{\mu'\mu\tau\tau'}^{VV'}(\pi - \theta) \quad , \quad (6)$$

while VV' -exchange implies

$$F_{\mu\mu'\tau\tau'}^{VV'}(\theta) = F_{\mu\mu'\tau'\tau}^{VV'}(\pi - \theta) \quad , \quad (7)$$

for all VV' -channels.

CP invariance for $VV' = \gamma\gamma, \gamma Z, ZZ$, gives

$$F_{\mu\mu'\tau\tau'}^{VV'}(\theta) = (-1)^{\tau-\tau'} F_{-\mu, -\mu', -\tau, -\tau'}^{VV'}(\theta) \quad , \quad (8)$$

while for the charged channel W^+W^- we get

$$F_{\mu\mu'\tau\tau'}^{W^+W^-}(\theta) = (-1)^{\tau-\tau'} F_{\mu'\mu\tau\tau'}^{W^+W^-}(\pi - \theta) = F_{-\mu', -\mu, -\tau', -\tau}^{W^+W^-}(\theta) \quad . \quad (9)$$

In addition, at the 1loop level, we find

$$F_{+++-}^{W^+W^-}(\theta) = F_{+-+-}^{W^+W^-}(\theta) \quad . \quad (10)$$

Combining (6, 7) for the $\gamma\gamma$ -channel, we get⁴

$$F_{\mu\mu'\tau\tau'}^{\gamma\gamma}(\theta) = F_{\mu'\mu\tau'\tau}^{\gamma\gamma}(\theta) \quad . \quad (11)$$

Correspondingly, for $gg \rightarrow ZZ$, the combination of (6, 7, 8), implies

$$\begin{aligned} F_{\mu\mu'\tau\tau'}^{ZZ}(\theta) &= (-1)^{\tau-\tau'} F_{\mu'\mu\tau\tau'}^{ZZ}(\pi - \theta) \quad , \\ F_{\mu\mu'\tau\tau'}^{ZZ}(\theta) &= F_{\mu\mu'\tau'\tau}^{ZZ}(\pi - \theta) \quad , \\ F_{\mu\mu'\tau\tau'}^{ZZ}(\theta) &= (-1)^{\tau-\tau'} F_{\mu'\mu\tau'\tau}^{ZZ}(\theta) \quad , \\ F_{\mu\mu'\tau\tau'}^{ZZ}(\theta) &= (-1)^{\tau-\tau'} F_{-\mu-\mu'-\tau-\tau'}^{ZZ}(\theta) \quad . \end{aligned} \quad (12)$$

⁴In addition to it, there exists also a photon-gluon symmetry, because of their common γ_μ -coupling.

These symmetries constrain the number of independent helicity amplitudes of the various processes $gg \rightarrow VV'$. Below we enumerate these independent amplitudes, conveniently separating them in three classes. The helicity conserving (HC) amplitudes that respect (2); the helicity violating TT and LL amplitudes, ($HV_{TT,LL}$) that violate (2); and finally the transverse-longitudinal HV_{TL} and HV_{LT} , which also violate (2).

As a result, for $gg \rightarrow \gamma\gamma$, there are 4 independent helicity amplitudes, namely

$$\begin{aligned} HC &\Rightarrow F_{++++}^{\gamma\gamma}(\theta) , \quad F_{+--+}^{\gamma\gamma}(\theta) = F_{+--+}^{\gamma\gamma}(\pi - \theta) , \\ HV_{TT} &\Rightarrow F_{++--}^{\gamma\gamma}(\theta) , \quad F_{++--}^{\gamma\gamma}(\theta) = F_{++--}^{\gamma\gamma}(\theta) = F_{++--}^{\gamma\gamma}(\theta) = F_{++--}^{\gamma\gamma}(\theta) . \end{aligned} \quad (13)$$

Correspondingly, for $gg \rightarrow \gamma Z$, we take as independent the 9 amplitudes

$$\begin{aligned} HC &\Rightarrow F_{++++}^{\gamma Z}(\theta) , \quad F_{+--+}^{\gamma Z}(\theta) = F_{+--+}^{\gamma Z}(\pi - \theta) , \\ HV_{TT} &\Rightarrow F_{+++-}^{\gamma Z}(\theta) , \quad F_{+++-}^{\gamma Z}(\theta) , \quad F_{+++-}^{\gamma Z}(\theta) , \quad F_{+++-}^{\gamma Z}(\theta) = F_{+++-}^{\gamma Z}(\pi - \theta) , \\ HV_{TL} &\Rightarrow F_{+++0}^{\gamma Z}(\theta) , \quad F_{+++0}^{\gamma Z}(\theta) , \quad F_{+++0}^{\gamma Z}(\theta) = F_{+++0}^{\gamma Z}(\pi - \theta) . \end{aligned} \quad (14)$$

For $gg \rightarrow ZZ$, (12) implies 10 independent amplitudes taken as

$$\begin{aligned} HC &\Rightarrow F_{++++}^{ZZ}(\theta) , \quad F_{+--+}^{ZZ}(\theta) = F_{+--+}^{ZZ}(\pi - \theta) , \quad F_{+-00}^{ZZ}(\theta) , \\ HV_{TT,LL} &\Rightarrow F_{+++-}^{ZZ}(\theta) , \quad F_{+++-}^{ZZ}(\theta) , \quad F_{+++-}^{ZZ}(\theta) , \quad F_{++00}^{ZZ}(\theta) \\ HV_{TL} &\Rightarrow F_{+++0}^{ZZ}(\theta) , \quad F_{+++0}^{ZZ}(\theta) , \quad F_{+++0}^{ZZ}(\theta) . \end{aligned} \quad (15)$$

Finally for $gg \rightarrow W^+W^-$, the combination of (6, 9, 10), implies 14 independent amplitudes for which we take

$$\begin{aligned} HC &\Rightarrow F_{++++}^{W^+W^-}(\theta) , \quad F_{+--+}^{W^+W^-}(\theta) , \quad F_{+--+}^{W^+W^-}(\theta) , \quad F_{+-00}^{W^+W^-}(\theta) , \\ HV_{TT,LL} &\Rightarrow F_{+++-}^{W^+W^-}(\theta) , \quad F_{+++-}^{W^+W^-}(\theta) , \quad F_{+++-}^{W^+W^-}(\theta) , \quad F_{++00}^{W^+W^-}(\theta) , \\ HV_{TL} &\Rightarrow F_{+++0}^{W^+W^-}(\theta) , \quad F_{+++0}^{W^+W^-}(\theta) , \quad F_{+++0}^{W^+W^-}(\theta) , \quad F_{+++0}^{W^+W^-}(\theta) , \\ HV_{LT} &\Rightarrow F_{++0+}^{W^+W^-}(\theta) , \quad F_{++0-}^{W^+W^-}(\theta) . \end{aligned} \quad (16)$$

The analytic results derived from Fig.1, are used to construct the Fortran code released together with this paper, which calculates all helicity amplitudes.

3 Asymptotic behavior of $F_{\mu\mu'\tau\tau'}$ in SM and MSSM.

In this Section we give the analytic asymptotic expressions for all 1loop independent helicity amplitudes for the processes in (3). These are valid at very high energies and fixed angles, in both SM and MSSM. For MSSM this means $\sqrt{s} \gg M_{SUSY}$, with M_{SUSY} describing the scale of the squark masses, and satisfying $M_{SUSY} \sim 1$ TeV, for the benchmarks [13, 14, 15, 16, 17]. For SM, $\sqrt{s} \gg m_W$ is sufficient.

It turns out that in MSSM, all HV amplitudes (HV_{TT} , HV_{LL} and HV_{TL}) indeed vanish asymptotically, while the HC ones tend to non-vanishing, angle-dependent "constants".

In SM, the HC amplitudes continue to behave like angle-dependent "constants" asymptotically. But in this case, the HV_{TT} and HV_{LL} amplitudes are also non-vanishing asymptotically, behaving like real constants, independent of the angle. The HV_{TL} -amplitudes continue to tend to a vanishing limit in⁵ SM (as they were also doing in MSSM).

So we only need to discuss the "constant" limits of the TT and LL amplitudes. These may be directly obtained from the analytical results for the graphs in Fig.1 in terms of the Passarino-Veltman functions [25], using the asymptotic expressions given e.g in [26]. Alternatively, for $VV' = \gamma\gamma$, γZ , ZZ , these may be obtained from the $\gamma\gamma$ -fusion results of [10, 8, 9]. For the WW case though, some extra work had to be done, particularly concerning the proof that the γ_5 contribution of the $F + H$ boxes in Fig.1, indeed vanishes asymptotically. Having done this, the values of the aforementioned limits, (which fully agree with the results of the 1loop code [23]) have been obtained. They are presented below, separating the TT and LL amplitudes:

The TT-amplitudes

Their general structure for all $gg \rightarrow VV'$ processes in MSSM has the form [10]

$$F_{\mu\mu'\tau\tau'} \rightarrow \frac{\alpha\alpha_s}{2} C_{VV'q} [f_{\mu\mu'\tau\tau'}^q + 2f_{\mu\mu'\tau\tau'}^{\bar{q}}] \quad , \quad (17)$$

where f^q and $f^{\bar{q}}$ denote respectively the V -independent part of the asymptotic quark and squark box loop contributions. Expression (17) may also be used for SM calculations, provided the $f^{\bar{q}}$ -term is dropped.

The relative magnitudes of the various processes in (17) is solely determined by the relevant couplings [10]

$$C_{VV'q} = \frac{1}{2} \sum_{\text{flavors}} [g_{Vq}^L g_{V'q}^L + g_{Vq}^R g_{V'q}^R] \quad , \quad (18)$$

where the summation is over all quark flavors. For three quark-generations, we thus find

$$C_{ZZq} = \frac{(9 - 18s_W^2 + 20s_W^4)}{12s_W^2 c_W^2} \quad , \quad C_{\gamma Zq} = \frac{(9 - 20s_W^2)}{12s_W c_W} \quad , \quad C_{\gamma\gamma q} = \frac{15}{9} \quad , \quad C_{WWq} = \frac{3}{4s_W^2} \quad , \quad (19)$$

for $gg \rightarrow ZZ$, γZ , $\gamma\gamma$, and W^+W^- , respectively.

The explicit expressions for the f^q , $f^{\bar{q}}$ in (17) are [10]

$$f_{\mu\mu'\tau\tau'}^q = -2A_{\mu\mu'\tau\tau'}^S + \delta_{\mu\mu'\tau\tau'} \quad , \quad f_{\mu\mu'\tau\tau'}^{\bar{q}} = A_{\mu\mu'\tau\tau'}^S \quad , \quad (20)$$

⁵By the equivalence theorem, this result is identical to the asymptotic vanishing of the $gg \rightarrow VG$ amplitudes found in [18] and induced by a mass suppression appearing already at the trace computation.

where the only non-vanishing contributions are

$$\begin{aligned}
A_{++++}^S &= A_{----}^S = 4 - \frac{4ut}{s^2} \left[\ln^2 \left| \frac{t}{u} \right| + \pi^2 \right] + \frac{4(t-u)}{s} \ln \left| \frac{t}{u} \right| , \\
A_{+--+}^S &= A_{-++-}^S = 4 - \frac{4st}{u^2} \left[\ln^2 \left| \frac{s}{t} \right| - 2i\pi \ln \left| \frac{s}{t} \right| \right] + \frac{4(s-t)}{u} \left[\ln \left| \frac{s}{t} \right| - i\pi \right] , \\
A_{+---}^S &= A_{-++-}^S = 4 - \frac{4su}{t^2} \left[\ln^2 \left| \frac{s}{u} \right| - 2i\pi \ln \left| \frac{s}{u} \right| \right] + \frac{4(s-u)}{t} \left[\ln \left| \frac{s}{t} \right| - i\pi \right] , \quad (21) \\
\delta_{++++} &= \delta_{----} = -4 \left[\ln^2 \left| \frac{u}{t} \right| + \pi^2 \right] , \\
\delta_{+--+} &= \delta_{-++-} = \delta^t \equiv -4 \left[\ln^2 \left| \frac{s}{t} \right| - i 2\pi \ln \left| \frac{s}{t} \right| \right] , \\
\delta_{+---} &= \delta_{-++-} = \delta^u \equiv -4 \left[\ln^2 \left| \frac{s}{u} \right| - i 2\pi \ln \left| \frac{s}{u} \right| \right] , \quad (22)
\end{aligned}$$

for the HC_{TT} amplitudes, and

$$\begin{aligned}
A_{++++}^S &= A_{+--+}^S = A_{+---}^S = A_{-++-}^S = A_{-+-+}^S = A_{----}^S = A_{-++-}^S = A_{+---}^S \\
&= A_{-++-}^S = A_{-++-}^S = A_{-++-}^S = -4 , \quad (23)
\end{aligned}$$

for the HV_{TT} amplitudes. Note that the substitution of $t = -s(1 - \cos \theta)/2$ and $u = -s(1 + \cos \theta)/2$ in the asymptotic relations (21, 22), provides consistent equivalent expressions in terms of θ .

Substituting (19-23) in (17), one observes that in MSSM, the squark contributions $f^{\tilde{q}} = A^S$ cancels out the A^S part of the quark boxes, so that non-vanishing contributions can only arise from the δ -terms in (22). Therefore, only the HC amplitudes F_{+--+} , F_{-++-} , F_{+---} , F_{-++-} , F_{++++} and F_{----} survive asymptotically, acquiring energy-independent, but angle-dependent values. A compact form of them may be written as

$$\begin{aligned}
F(gg \rightarrow ZZ)_{\mu\mu'\tau\tau'}^{\text{as}} &= \alpha\alpha_s \frac{(9 - 18s_W^2 + 20s_W^4)}{24s_W^2 c_W^2} \delta_{\mu\mu'\tau\tau'} , \\
F(gg \rightarrow \gamma Z)_{\mu\mu'\tau\tau'}^{\text{as}} &= \alpha\alpha_s \frac{(9 - 20s_W^2)}{24s_W c_W} \delta_{\mu\mu'\tau\tau'} , \\
F(gg \rightarrow \gamma\gamma)_{\mu\mu'\tau\tau'}^{\text{as}} &= \alpha\alpha_s \frac{5}{6} \delta_{\mu\mu'\tau\tau'} , \\
F(gg \rightarrow W^+W^-)_{\mu\mu'\tau\tau'}^{\text{as}} &= \alpha\alpha_s \frac{3}{8s_W^2} \delta_{\mu\mu'\tau\tau'} , \quad (24)
\end{aligned}$$

in terms of (22).

On the contrary, in SM there are no squarks, so that only the quark box contribution $f^q = -2A^S + \delta$ must be retained in (17, 20). Using then (21-23), we obtain non-vanishing asymptotic limits for all the HC_{TT} and the HV_{TT} amplitudes. The HC_{TT} limits continue to depend on the angle; see (21, 22). But HV_{TT} amplitudes in SM, all tend to the same constant value, independent of the scattering angle θ ; see(23).

The LL-amplitudes

These asymptotic limits only concern the $gg \rightarrow Z_L Z_L$, $W_L^+ W_L^-$ amplitudes, which should be equivalent to $gg \rightarrow G^0 G^0$, $G^+ G^-$ respectively [19, 20, 21].

In SM, non vanishing "constant" limits are found for both, the HC_{LL} amplitudes [10, 18]

$$\begin{aligned} F_{+-00}^{ZZ}(\theta) &= F_{-+00}^{ZZ}(\theta) \rightarrow \alpha\alpha_s \frac{(m_t^2 + m_b^2)}{16s_W^2 m_W^2} \left\{ \delta^t \frac{(1 - \cos \theta)}{1 + \cos \theta} + \delta^u \frac{(1 + \cos \theta)}{1 - \cos \theta} \right\} , \\ F_{+-00}^{W^+ W^-}(\theta) &= F_{-+00}^{W^+ W^-}(\pi - \theta) \rightarrow \frac{\alpha\alpha_s}{8s_W^2 m_W^2} \left\{ \delta^t \frac{m_b^2 (1 - \cos \theta)}{1 + \cos \theta} + \delta^u \frac{m_t^2 (1 + \cos \theta)}{1 - \cos \theta} \right\} \end{aligned} \quad (25)$$

where δ^t, δ^u are defined in (22); and the HV_{LL} amplitudes

$$\begin{aligned} F_{++00}^{ZZ}(\theta) &= F_{--00}^{ZZ}(\theta) \rightarrow -\alpha\alpha_s \frac{(m_t^2 + m_b^2)}{s_W^2 m_W^2} \\ F_{++00}^{WW}(\theta) &= F_{--00}^{WW}(\pi - \theta) \rightarrow -\alpha\alpha_s \frac{(m_t^2 + m_b^2)}{s_W^2 m_W^2} . \end{aligned} \quad (26)$$

In MSSM, the HV_{LL} amplitudes F_{++00}^{ZZ} , F_{++00}^{WW} vanish because of squark/quark cancellations; while the HC_{LL} limits in (25) continue to hold, due to the vanishing of the asymptotic squark-loop contributions.

It is worth emphasizing at this point that in both, MSSM and SM, the asymptotic limits of the TT amplitudes depend solely on the gauge couplings; while the LL ones depend in addition on the top and bottom masses⁶.

It is moreover impressive to observe the SM HV_{TT} and HV_{LL} amplitudes to tend asymptotically to real constants, which in MSSM are exactly canceled by opposite squark contributions, due to the beautiful HCns theorem.

Note that the behavior of the HV_{LL} amplitudes F_{++00}^{ZZ} , F_{++00}^{WW} is related by the equivalence theorem [19, 20, 21], to the Goldstone amplitudes discussed in [18]. The HV_{TT} results though, are new and indicate strong violation of HCns in 12 independent SM amplitudes; compare (13-16).

The approach to the limiting values of the various $gg \rightarrow VV'$ amplitudes mentioned above, appears like m/\sqrt{s} or m^2/s , multiplied by logarithms. Therefore, the asymptotic limits should be reached rather early; i.e. as soon as the energy exceeds by a few times m_W in SM, or M_{SUSY} in MSSM.

The limits (17), may be used to derive the asymptotic relation

$$\begin{aligned} \frac{F_{\mu\mu'\tau\tau'}(gg \rightarrow \gamma\gamma)}{C_{\gamma\gamma q}} &= \frac{F_{\mu\mu'\tau\tau'}(gg \rightarrow \gamma Z)}{C_{\gamma Z q}} \\ &= \frac{F_{\mu\mu'\tau\tau'}(gg \rightarrow ZZ)}{C_{ZZ q}} = \frac{F_{\mu\mu'\tau\tau'}(gg \rightarrow W^+ W^-)}{C_{WW q}} , \end{aligned} \quad (27)$$

⁶We neglect the quark masses of the first two generations in this work.

for the HC_{TT} amplitudes in MSSM, and all TT-amplitudes in SM.

In MSSM, where all other amplitudes vanish asymptotically, (27) may be transformed to asymptotic relations among unpolarized cross sections, by subtracting the LL-parts of the $gg \rightarrow VV'$ -processes, using the R_1, R_2, R_3 relations of [18] and the equivalence theorem [19, 20, 21]. This way, in addition to the seven relations (R_1, \dots, R_7) derived in [18], we obtain

$$\begin{aligned}
R_8 \Rightarrow \frac{\tilde{\sigma}(gg \rightarrow \gamma\gamma)}{C_{\gamma\gamma q}^2} &= \frac{\tilde{\sigma}(gg \rightarrow \gamma Z)}{C_{\gamma Z q}^2} = \frac{\left[\tilde{\sigma}(gg \rightarrow ZZ) - \left(\frac{R_{a1}}{R_{a5}} \right)^2 \tilde{\sigma}(gg \rightarrow h^0 h^0) \right]}{C_{ZZq}^2} \\
&= \frac{\left[\tilde{\sigma}(gg \rightarrow W^+ W^-) - \left(\frac{R_{a1}}{R_{a5}} \right)^2 \tilde{\sigma}(gg \rightarrow h^0 h^0) - \left(\frac{R_{c1}^J}{R_{b2}} \right)^2 \tilde{\sigma}(gg \rightarrow Zh^0) \right]}{C_{WWq}^2} , \quad (28)
\end{aligned}$$

where we have used the "dimensionless" unpolarized differential cross sections

$$\tilde{\sigma}(gg \rightarrow VV') \equiv \frac{512\pi s^{3/2}}{\alpha^2 \alpha_s^2 p} \frac{d\sigma(gg \rightarrow VV'; s)}{d\cos\theta} = \sum_{\mu\mu'\tau\tau'} \frac{|F_{\mu\mu'\tau\tau'}^{VV'}|^2}{\alpha^2 \alpha_s^2} , \quad (29)$$

and correspondingly for the $h^0 h^0$ and Zh^0 production processes. The constants needed in (28) are

$$\begin{aligned}
R_{a1} &= m_t^2 + m_b^2 , \quad R_{a5} = \frac{m_t^2 \cos^2 \alpha}{\sin^2 \beta} + \frac{m_b^2 \sin^2 \alpha}{\cos^2 \beta} , \\
R_{b2} &= \frac{m_t^2 \cos \alpha}{\sin \beta} + \frac{m_b^2 \sin \alpha}{\cos \beta} , \quad R_{c1}^J = m_t^2 - m_b^2 \simeq R_{a1} , \quad (30)
\end{aligned}$$

defined in [18], with α, β being the usual scalar sector angles in MSSM. Eqs.(19) is also used in (28).

Relation (28) is an asymptotic MSSM prediction involving measurable cross sections. It is on the same footing as the R_1, R_2, R_3, R_4, R_5 , relations listed in (23-27) of [18]. If MSSM is realized in Nature, their validity is guaranteed, provided the energy is sufficiently higher than the SUSY scale.

4 Numerical results in MSSM and SM

The asymptotic values of all TT and LL amplitudes for $gg \rightarrow VV'$ in SM and MSSM, only depend on the gauge couplings and the top and bottom masses; see Sect.3. The corresponding numerical results are given in Table 1. The longitudinal-transverse (HV_{TL}) asymptotic amplitudes are not presented, since they all vanish, for both MSSM and SM.

As seen from this Table, all HV amplitudes indeed asymptotically vanish in MSSM, in agreement with HCns.

Table 1: Asymptotic TT and LL Helicity Amplitudes divided by $\alpha\alpha_s$, and asymptotic $\tilde{\sigma}(gg \rightarrow VV')$, in MSSM and SM, at $\theta = 60^\circ$.

$gg \rightarrow \gamma\gamma$			$gg \rightarrow \gamma Z$		
	MSSM	SM		MSSM	SM
$F_{++++}(\theta)$	-37.	-26.	$F_{++++}(\theta)$	-19.	-13.5
$F_{+--+}(\theta)$	$-6.4 + i29$	$-3.4 + i20$	$F_{+--+}(\theta)$	$-3.3 + i15.$	$-1.7 + i10.3$
$F_{+---}(\theta)$	$-0.28 + i6.0$	$-0.14 + i4.0$	$F_{+---}(\theta)$	$-0.14 + i3.1$	$-0.07 + i2.1$
$F_{++--}(\theta)$	0	6.7	$F_{++--}(\theta)$	0	3.4
$F_{+++-}(\theta)$	0	6.7	$F_{+++-}(\theta)$	0	3.4
			$F_{++-+}(\theta)$	0	3.4
			$F_{+-++}(\theta)$	0	3.4
$\tilde{\sigma}(gg \rightarrow \gamma\gamma)$	4567	2654	$\tilde{\sigma}(gg \rightarrow \gamma Z)$	1220	709

$gg \rightarrow ZZ$			$gg \rightarrow W^+W^-$		
	MSSM	SM		MSSM	SM
$F_{++++}(\theta)$	-61	-43	$F_{++++}(\theta)$	-72.	-51.
$F_{+--+}(\theta)$	$-10.6 + i48.1$	$-5.6 + i33.$	$F_{+--+}(\theta)$	$-12. + i56.$	$-6.5 + i39$
$F_{+---}(\theta)$	$-0.46 + i10.$	$-0.23 + i6.7$	$F_{+---}(\theta)$	$-0.5 + i12.$	$-0.27 + i7.8$
$F_{++--}(\theta)$	0	11.	$F_{++--}(\theta)$	0	12.9
$F_{+++-}(\theta)$	0	11.	$F_{+++-}(\theta)$	0	12.9
$F_{+-++}(\theta)$	0	11.	$F_{+-++}(\theta)$	0	12.9
$F_{+-00}(\theta)$	$-4.6 + i43.$	$-4.6 + i43.$	$F_{+-00}(\theta)$	$-2.6 + i56.$	$-2.6 + i56.$
$F_{++00}(\theta)$	0	-20.5	$F_{++00}(\theta)$	0	-20.5
$\tilde{\sigma}(gg \rightarrow ZZ)$	16226	11820	$\tilde{\sigma}(gg \rightarrow W^+W^-)$	21232	14873

On the contrary for SM, the full number of the 12 independent HV_{TT} amplitudes and the two HV_{LL} ones, acquire non-vanishing asymptotic values, comparable to those of the HC amplitudes. Moreover, these SM asymptotic amplitudes only depend on the process; they are independent of the scattering angle and the specific helicities; see (19, 23, 26).

A further conclusion we can draw is that, contrary to the situation in $\gamma\gamma \rightarrow \gamma\gamma, \gamma Z, ZZ$, where HCNs is approximately satisfied in SM [8, 9, 10]; it is strongly violated in the $gg \rightarrow VV'$ SM amplitudes.

In the same Table, the asymptotic values for the "dimensionless" unpolarized differential cross sections defined in (29) are also given.

The analytic calculation of the diagrams in Fig.1 is used to construct the `ggvcode` Fortran code computing the helicity amplitudes of the processes (3) in SM and MSSM, as functions of the c.m. energy in TeV and the c.m. angle in radians. The amplitude conventions are given immediately after (4), while its overall normalization is fixed by (29). A factor $\alpha\alpha_s$ has been removed from the amplitudes, in the code-output. All input parameters are taken real and at the electroweak scale. The code, accompanied by a Readme file explaining its compilation and use, may be downloaded from [23]. The asymptotic limits presented in Table 1 agree with the results of the code.

Using this code we study in detail how the 1loop EW corrected amplitudes behave, as the energy increases. The results for these amplitudes are presented in figures bellow, the main goal of which is to show the differences between SM and MSSM. Thus, in Figs.2,3 we present the HC and $HV_{TT,LL}$ independent helicity amplitudes for $gg \rightarrow W^+W^-$, defined in (16). The corresponding ones for $gg \rightarrow ZZ$, are shown in Figs.4, 5 using (15); while in Figs.6, 7, the HC and HV_{TT} independent amplitudes for $gg \rightarrow \gamma Z$ are shown using (14).

In all these cases, left panels give the $SPS1a'$ MSSM result [13], and right panels the SM one. The upper panels always describe the energy distributions, while the lower panels give the angular distributions. Note that the sensitivity of the MSSM result on the specific benchmark, is only at intermediate energies. The high energy limit is independent of it; while at energies much below M_{SUSY} , all MSSM amplitudes coincide with the SM ones .

No amplitudes for $gg \rightarrow \gamma\gamma$ are shown, since their structure is very similar to the $gg \rightarrow \gamma Z$ results, apart from the overall scale factors; compare (27, 19).

As seen in Figs.2, 4, 6, the shapes of the various HC amplitudes in MSSM ($SPS1a'$) and SM, are rather similar, for all processes (3), while their asymptotic values are reached at energies $\lesssim 4TeV$.

The differences between MSSM and SM become striking though, for the $HV_{TT,LL}$ amplitudes in Figs.3, 5, 7. In MSSM (left panels) they vanish quickly like

$$\begin{aligned} F_{++++} &\simeq F_{+---} \sim \frac{m}{\sqrt{s}} \log^n s \quad , \\ |F_{++++}| &\gtrsim |F_{++00}| \gtrsim |F_{++--}| \sim \frac{m^2}{s} \log^{n'} s \quad , \end{aligned} \quad (31)$$

for $gg \rightarrow W^+W^-$, ZZ ; while for $gg \rightarrow \gamma Z$ they behave as

$$F_{++++} \simeq F_{+---} \simeq F_{+--+} > |F_{++--}| \sim \frac{m^2}{s} \log^{n''} s \quad , \quad (32)$$

where n, n', n'' are numbers.

In SM (right panels of Figs.3, 5, 7) all $HV_{TT,LL}$ amplitudes go to constant, angle-independent limits, as required by (17, 23, 26). Moreover, for $gg \rightarrow W^+W^-$, ZZ , the F_{++00} amplitude is the largest one, above $\sim 2TeV$. This is also confirmed by Table 1.

We next turn to the TL or LT amplitudes, which vanish at high energies, in both MSSM and SM. The difference between the MSSM and SM predictions for these amplitudes is very small, for all energies. Therefore, we only show MSSM results here.

In Figs.8 we present the TL (left panels) and LT (right panels) amplitudes for $gg \rightarrow W^+W^-$ for ($SPS1a'$). The upper panels give the energy distributions, while the lower panels give the angular distributions at $\sqrt{s} = 10TeV$. As seen there, all these amplitudes vanish quickly, with increasing energy; while $F_{++0-}^{WW}(\theta) \simeq -F_{++-0}^{WW}(\theta) \simeq 0$ at almost all energies.

A similar behavior is observed in Figs.9 presenting the HV_{TL} amplitudes for $gg \rightarrow ZZ$, with the left panel giving the energy distributions, and the right panel the angular ones, always in MSSM. Again $F_{++0-}^{ZZ}(\theta) = -F_{++-0}^{ZZ}(\theta) \simeq 0$ is found at almost all energies. The corresponding amplitudes for $gg \rightarrow \gamma Z$ vanish even faster, as the energy increases.

Concerning the angular dependencies of the various amplitudes appearing in Figs.2-9, we remark that their approach to asymptopia for the MSSM (*SPS1a'*) benchmark, reaches the 10% level, already at an energy of about 10 TeV, for a wide angular region. This is most convincingly seen by comparing the angular distributions for the dominant HC amplitudes in Figs.2, 4, 6, with the suppressed HV amplitudes in Figs.3, 5, 7, 8, 9.

In Fig.10 we present the "dimensionless" unpolarized differential cross sections defined in (29) for all four processes in (3). The panels of the first row refer to the WW -channel, those of the middle one to the ZZ -channel, and finally those of the third row to the γZ and $\gamma\gamma$ channels. In each row, the left panels give the energy dependence for a fixed angle $\theta = 60^\circ$, in both *SPS1a'* of MSSM [13] and in SM. Correspondingly, the right panels give the angular dependencies in radians, at c.m. energies 1 and 10TeV for WW and ZZ , but only at 10TeV for $\gamma\gamma$ and γZ .

At very high energies ($s \gg M_{SUSY}^2$), the cross sections in Fig.10, only depend on the gauge couplings and the top and bottom masses; compare the asymptotic results in the Table. Nevertheless, the differences between the SM and MSSM predictions, even at very high energies, are quite large and of course independent of the MSSM benchmark. At $s \ll M_{SUSY}^2$, the SM and MSSM results should of course coincide. The only possible benchmark dependence may appear at energies comparable to M_{SUSY} , which of course, apart from the actual dependence on it, may also push the validity of the asymptotic predictions to higher or lower energies [13, 14, 15, 16, 17].

We are presently investigating other such asymptotic relations involving the unpolarized cross sections $\tilde{\sigma}(gg \rightarrow VV')$, $\tilde{\sigma}(gg \rightarrow \tilde{\chi}_i^+ \tilde{\chi}_j^-)$ and $\tilde{\sigma}(gg \rightarrow \tilde{\chi}_i^0 \tilde{\chi}_j^0)$ [27]. Some of these relations are found to be approximately correct even at LHC type energies, for *SPS1a'* [13] and similarly low SUSY scale benchmarks; much like it appeared for $ug \rightarrow dW^+$, $\tilde{d}_L \tilde{\chi}_i^+$ in [12]. There exist cross section relations though, like those involving the production of specific neutralino or chargino pairs, where much higher energies are needed for them to hold [27].

We next turn to what could eventually be the LHC implications of the extensive 1loop EW calculation for $gg \rightarrow VV'$, we have performed. To avoid any misunderstanding though, we emphasize that the reason we have performed this calculation was not in order to check its observability at LHC; but in order to improve our understanding of the beautiful helicity conservation property endowed to SUSY.

Having said this, the contribution to VV' production due to gluon fusion at LHC, may be written as

$$\frac{d\sigma(pp \rightarrow VV' \dots)}{ds d\cos\theta} = \frac{L_{gg}}{S} \frac{d\sigma(gg \rightarrow VV'; s)}{d\cos\theta} ,$$

$$L_{gg} = \int_0^1 \frac{dx_1}{x_1} g(x_1, Q^2) g\left(\frac{\tau}{x_1}, Q^2\right) \quad , \quad \tau = \frac{s}{S} \quad , \quad (33)$$

where $g(x, Q^2)$ is the gluon distribution function of the proton at an appropriate scale Q [28], s is the subprocess c.m. energy-squared, θ is the c.m. scattering angle, and S the LHC energy-squared. The relation of the $F_{\mu\mu'\tau\tau'}^{VV'}$ amplitudes to the cross sections appears in (29).

Relation (33) is the basic quantity determining the difference between SM and MSSM. Integrating for example over all angles, we get the invariant mass squared distributions $d\sigma(pp \rightarrow VV')/ds$ presented in the left panel of Fig.11, for $SPS1a'$ [13] and SM. In it we used $Q = \sqrt{s}$, and the MRST2006nnlo code for the gluon distribution function⁷ [28].

Correspondingly, in the right panel of Fig.11, we show the relative changes that MSSM creates to the SM predictions for $d\sigma(pp \rightarrow VV')/ds$. As seen there, the difference between the MSSM and the SM predictions at ~ 1 TeV, reaches the 30% level for the WW channel, while for the ZZ channel it approaches 70%. For the $\gamma\gamma$ and γZ channels, the effect is rather small. This is mainly due to the triangle graphs involving Higgs exchange in the s -channel, which are very important for the WW and ZZ channels (due to a large LL contribution), but absent in the γZ and $\gamma\gamma$ channels.

Integrating $d\sigma(pp \rightarrow VV')/ds$ for all invariant masses higher than 0.5, 1 or 2 TeV in SM and $SPS1a'$, we obtain the results of Table 2, indicating again an appreciable SUSY effect in the WW and ZZ channels, provided the SUSY scale is in the $SPS1a'$ -range.

Table 2: Gluon fusion contribution to the LHC VV' production cross section in SM, and the relative $SPS1a'$ MSSM effects, for various ranges of the subprocess energy \sqrt{s} .

	$\sigma(pp \rightarrow \gamma\gamma)_{gg}$		$\sigma(pp \rightarrow \gamma Z)_{gg}$	
	SM (fb)	($SPS1a'$ -SM)/SM	SM (fb)	($SPS1a'$ -SM)/SM
$\sqrt{s} > 0.5$ TeV	17.4	0.005	5.33	0.005
$\sqrt{s} > 1$ TeV	0.657	0.055	0.186	0.008
$\sqrt{s} > 2$ TeV	0.011	0.37	0.003	0.341
	$\sigma(pp \rightarrow ZZ)_{gg}$		$\sigma(pp \rightarrow W^+W^-)_{gg}$	
	SM (fb)	($SPS1a'$ -SM)/SM	SM (fb)	($SPS1a'$ -SM)/SM
$\sqrt{s} > 0.5$ TeV	64.9	0.239	77	0.125
$\sqrt{s} > 1$ TeV	2.35	0.417	3.09	0.224
$\sqrt{s} > 2$ TeV	0.039	0.232	0.052	0.266

The (20-30)% $SPS1a'$ effects for $gg \rightarrow ZZ$, W^+W^- in Fig.11 and Table 2, may be observable at LHC and interesting; note that the QCD and parton-distribution uncertainties are usually less than 10%. For concrete predictions though, a detail collider simulation study is needed, including the potentially much larger $q\bar{q} \rightarrow VV'$ subprocess cross section and a background study, using appropriate LHC cuts. Such a study is much beyond the scope of the present work.

⁷Very similar results are expected for e.g the lowest order gluon distributions MRST2004lo of [28] also.

5 Summary and future developments

In the present work, we have made a complete 1loop computation of the electroweak contributions to the processes $gg \rightarrow \gamma\gamma, \gamma Z, ZZ, W^+W^-$. Since there is no Born terms to these, their amplitudes reflect deeply the features of the electroweak dynamics.

These amplitudes are divided into two classes; the helicity conserving (HC) ones that in MSSM respect HCns, and the helicity violating (HV) ones, that violate it. We have calculated them in SM and MSSM, and a numerical code is released, which gives all amplitudes as functions of the c.m energy and angle. All input parameters are assumed real and taken at the EW scale [23]..

In addition, simple analytic expressions for all asymptotic amplitudes in SM and MSSM, have been established, which are valid up to small corrections $\mathcal{O}(m/\sqrt{s})$ or $\mathcal{O}(m^2/s)$. These expressions depend only on the gauge couplings and the top and bottom masses. For the HC amplitudes in particular, they are energy-independent, but depend on the scattering angle, in both MSSM and SM.

In MSSM, all HV amplitudes of course vanish asymptotically, and HCns is respected.

But in SM, only the TL and LT amplitudes tend to zero at high energies. All the TT and LL helicity violating amplitudes become asymptotically real constants, independent of the c.m. angle, and comparable in magnitude to the HC ones. There are twelve independent such TT amplitudes, and two LL ones, indicating that HCns is strongly violated in SM for $gg \rightarrow \gamma\gamma, \gamma Z, ZZ, W^+W^-$.

In [18] we have seen such a strong violation of HCns in SM, but it only affected amplitudes related by the equivalence theorem to the two LL above [19, 20, 21]. The HCns violation for the transverse HV amplitudes presented here, is a new result involving many more amplitudes.

The HCns validity in MSSM for transverse amplitudes were previously seen in $\gamma\gamma \rightarrow \gamma\gamma, \gamma Z, ZZ$ processes, [8, 9, 10]; but in that case, the W loop dominance allowed one to infer that helicity conservation is approximately true in SM also. An inference supported also by all processes enjoying a non-vanishing Born contribution.

It is only in the present study of $gg \rightarrow \gamma\gamma, \gamma Z, ZZ, W^+W^-$, that a strong violation of HCns has been seen in SM, for amplitudes involving transverse electroweak bosons.

As seen from the figures, at very high energies the SM and MSSM amplitudes and cross sections are considerably or even spectacularly different. In fact, at such energies the difference between SM and MSSM solely arises from the quantum numbers of the virtual particles participating in the loops; quarks in SM, and quarks+squarks in MSSM, with their masses and mixings being irrelevant. So $gg \rightarrow VV'$ at very high energy simply measure the quark and squark degrees of freedom, and can only depend on the gauge couplings, as we have found above.

Intermediate energies comparable to the SUSY scale, is the place where the differences between SM and MSSM predictions depend also on the SUSY masses and mixing parameters. These differences originate from all possible amplitudes, TT, LL and TL or LT. They affect both, the magnitude and the angular distribution of the cross sections. The ggvvcode released here, may be used to study such effects for gluon fusion to EW gauge

bosons.

When some SUSY masses will hopefully be discovered at LHC, the above code, as well as the corresponding one released in [18], may be used to indicate how the actual $gg \rightarrow VV', HH', VH$ amplitudes compare to their asymptotic helicity conserving values. In fact, it is through such codes, and the corresponding ones released in [4, 12], that the non-asymptotic implications of the physics leading to the HCns theorem [1, 2], may be assessed.

A nice way to understand the meaning of HCns [1, 2], is to relate it to the old Coleman-Mandula theorem [29], which was claiming that any attempt to combine non trivially the Poincaré and internal symmetries, would necessarily lead to vanishing amplitudes for all processes. The only known way to evade this theorem is supersymmetry; but not without a price. And the price SUSY has paid, is to have most of its 2-to-2 amplitudes vanishing asymptotically⁸. Only the few helicity conserving ones can survive in this limit [1, 2].

Up to now, in all our MSSM studies, we have assumed R-parity conservation. It should be straightforward to extend HCns to any non-minimal SUSY model in four dimensions, provided renormalizability is respected. Renormalizability seems necessary for the validity of HCns. All known non-renormalizable couplings violate it, already at the tree level [3]. The validity of HCns in cases where R-parity is violated, needs to be investigated.

Acknowledgements GJG is partially supported by the European Union contract MRTN-CT-2006-035505 HEPTOOLS, and the European Union ITN programme "UNILHC" PITN-GA-2009-237920. Discussions with G. Altarelli are gratefully acknowledged.

References

- [1] G.J. Gounaris and F.M. Renard, Phys. Rev. Lett. **94**, 131601 (2005), hep-ph/0501046.
- [2] G.J. Gounaris and F.M. Renard, Phys. Rev. **D73**, 097301 (2006), hep-ph/0604041, (an Addendum).
- [3] G.J. Gounaris, Acta Phys. Polon. **B37**, 1111 (2006), hep-ph/0510061.
- [4] G.J. Gounaris, J. Layssac and F.M. Renard, Phys. Rev. **D77**, 013003 (2008), arXiv:0709.1789 [hep-ph].
- [5] M. Beccaria, F.M. Renard and C. Verzegnassi, hep-ph/0203254, "Logarithmic Fingerprints of Virtual Supersymmetry", Linear Collider note LC-TH-2002-005, GDR Supersymmetrie note GDR-S-081.

⁸The "asymptotic" specification is easily understood, since we must avoid the effects that softly break the symmetry.

- [6] M. Beccaria, M. Melles, F. M. Renard, S. Trimarchi, C. Verzegnassi, *Int. J. Mod. Phys.* **A18**, 5069 (2003), hep-ph/0304110.
- [7] M. Beccaria, F.M. Renard and C. Verzegnassi, *Int. J. Mod. Phys.* **A23**, 1839 (2008), arXiv:0904.2646[hep-ph].
- [8] G.J. Gounaris, P.I. Porfyriadis and F.M. Renard, *Eur. Phys. J.* **C9**, 673 (1999), arXiv:hep-ph/9902230.
- [9] G.J. Gounaris, J. Layssac, P.I. Porfyriadis and F.M. Renard, *Eur. Phys. J.* **C10**, 499 (1999), arXiv:hep-ph/9904450.
- [10] G.J. Gounaris, J. Layssac, P.I. Porfyriadis and F.M. Renard, *Eur. Phys. J.* **C13**, 79 (2000), arXiv:hep-ph/9909243.
- [11] G.J. Gounaris, J. Layssac, P.I. Porfyriadis and F.M. Renard, *Eur. Phys. J.* **C19**, 57 (2001), arXiv:hep-ph/00100006.
- [12] G.J. Gounaris, J. Layssac and F.M. Renard, *Phys. Rev.* **D77**, 093007 (2008), arXiv:0803.0813 [hep-ph].
- [13] J.A. Aguilar-Saavedra et al., SPA convention, *Eur. Phys. J.* **C46**, 43 (2005), hep-ph/0511344.
- [14] B.C. Allanach et al. *Eur. Phys. J.* **C25**, 113 (2002), hep-ph/0202233.
- [15] H. Baer, V. Barger, G. Shaughnessy, H. Summy and L-T Wang, hep-ph/0703289.
- [16] D. Feldman, Z. Liu and P. Nath, *Phys. Rev. Lett.* **99**, 251802 (2007), arXiv:0707.1873 [hep-ph]
- [17] D. Feldman, Z. Liu and P. Nath, arXiv:0802.4085.
- [18] G.J. Gounaris, J. Layssac and F.M. Renard, arXiv: 0903.4532 [hep-ph], *Phys. Rev.* **D80**, 013009 (2009).
- [19] J.M. Cornwall, D.N. Levin, and G. Tiktopoulos, *Phys. Rev.* **D10**, 1145 (1974).
- [20] M.S. Chanowitz, and M.K. Gaillard, *Nucl. Phys.* **B261**, 379 (1985).
- [21] G.J. Gounaris, R. Kögerler and H. Neufeld, *Phys. Rev.* **D34**, 3257 (1986).
- [22] M.S. Berger and Chung Kao, *Phys. Rev.* **D59**, 075004 (1999), arXiv:9809240 [hep-ph] and references therein.
- [23] The ggvcodes FORTRAN codes together with a Readme file explaining its use, are contained in <http://users.auth.gr/gounaris/FORTRANcodes>. All input parameters in the code are at the electroweak scale.

- [24] M. Jacob and G.C. Wick, *Annals of Phys.* **7**, 404 (1959), *Annals of Phys.* **281**, 774 (2000)
- [25] G. Passarino and M. Veltman *Nucl. Phys.* **B160**, 151 (1979).
- [26] M. Beccaria, G.J. Gounaris, J. Layssac and F.M. Renard, *Int. J. Mod. Phys.* **A23**, 1839 (2008), arXiv:0711.1067 [hep-ph].
- [27] G.J. Gounaris, J. Layssac and F.M. Renard, in preparation..
- [28] A. D. Martin, W. J. Stirling, R. S. Thorne and G. Watt, "Update of Parton Distributions at NNLO", arXiv:0706.0459 [hep-ph], *Phys.Lett.B*652:292-299,2007.
- [29] S. Coleman and J. Mandula, *Phys. Rev.* **159**, 1251 (1967).

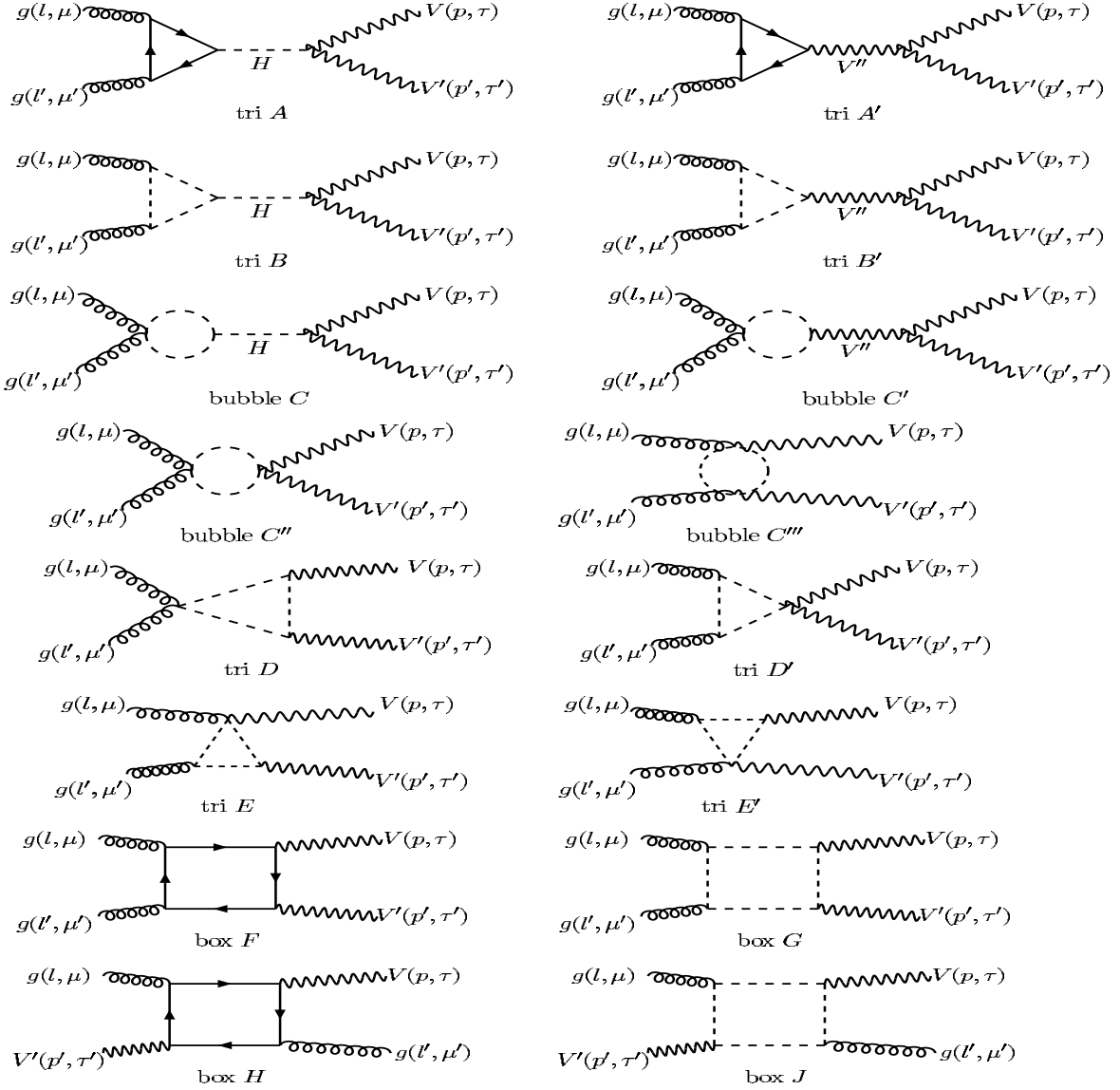


Figure 1: Independent EW contributing graphs to $gg \rightarrow VV'$. Full internal lines describe quark exchanges, while broken lines denote squark exchanges. The Higgs H exchanges in the graphs tri-A, tri-B and tri-C, are also denoted by broken lines. V, V', V'' denote the EW gauge bosons.

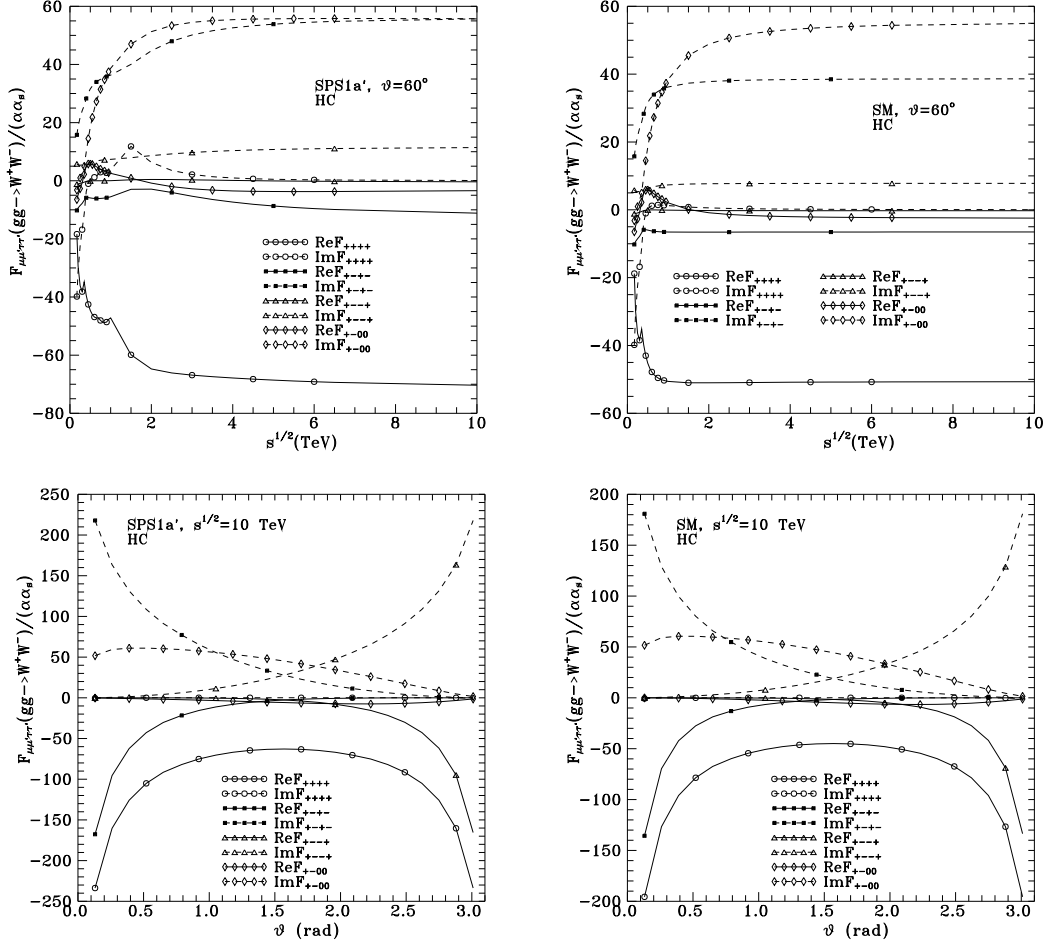


Figure 2: HC amplitudes for $gg \rightarrow W^+W^-$ in $SPS1a'$ and SM. Upper panels give the energy dependencies at a fixed c.m. angle $\theta = 60^\circ$; while lower panels give the angular distributions for a c.m. energy $\sqrt{s} = 10 \text{ TeV}$. Left panels always give the MSSM ($SPS1a'$) result [13], while right panels the SM one.

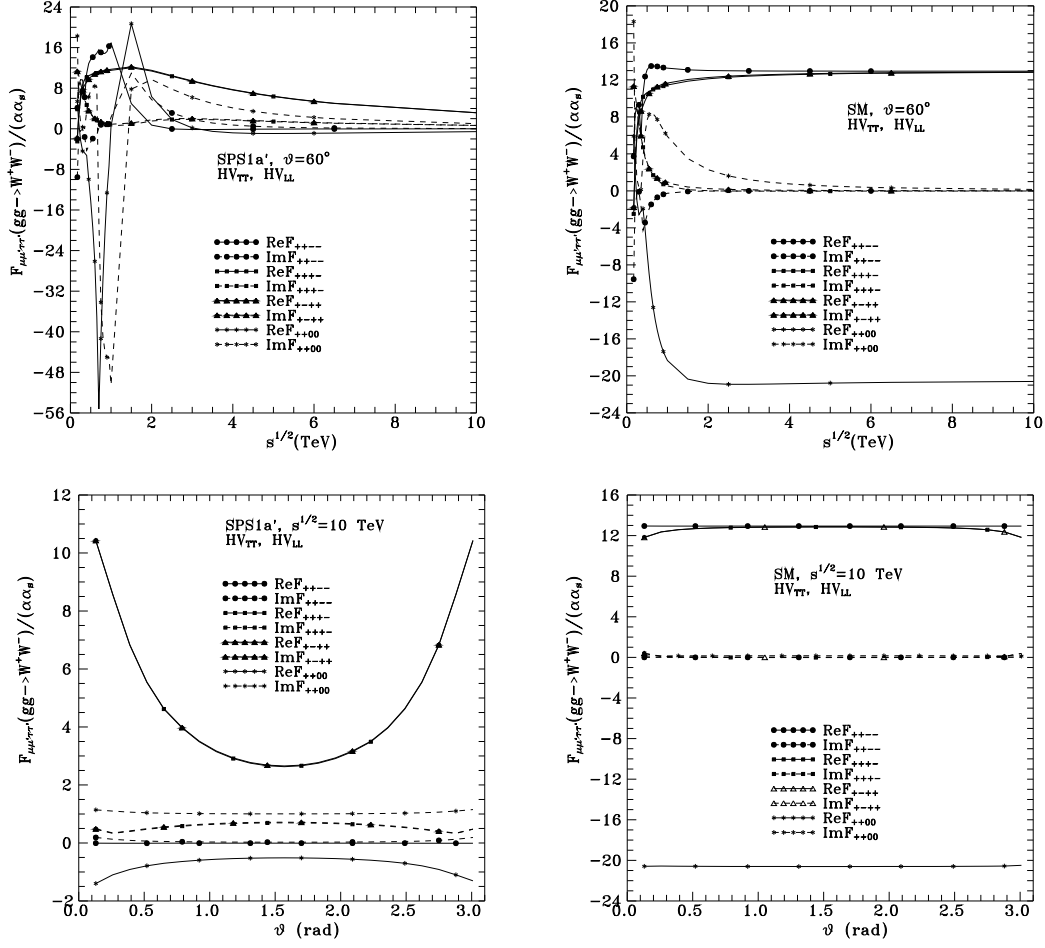


Figure 3: HV_{TT} and HV_{LL} amplitudes for $gg \rightarrow W^+W^-$ in $SPS1a'$ and SM, as in Fig. 2.

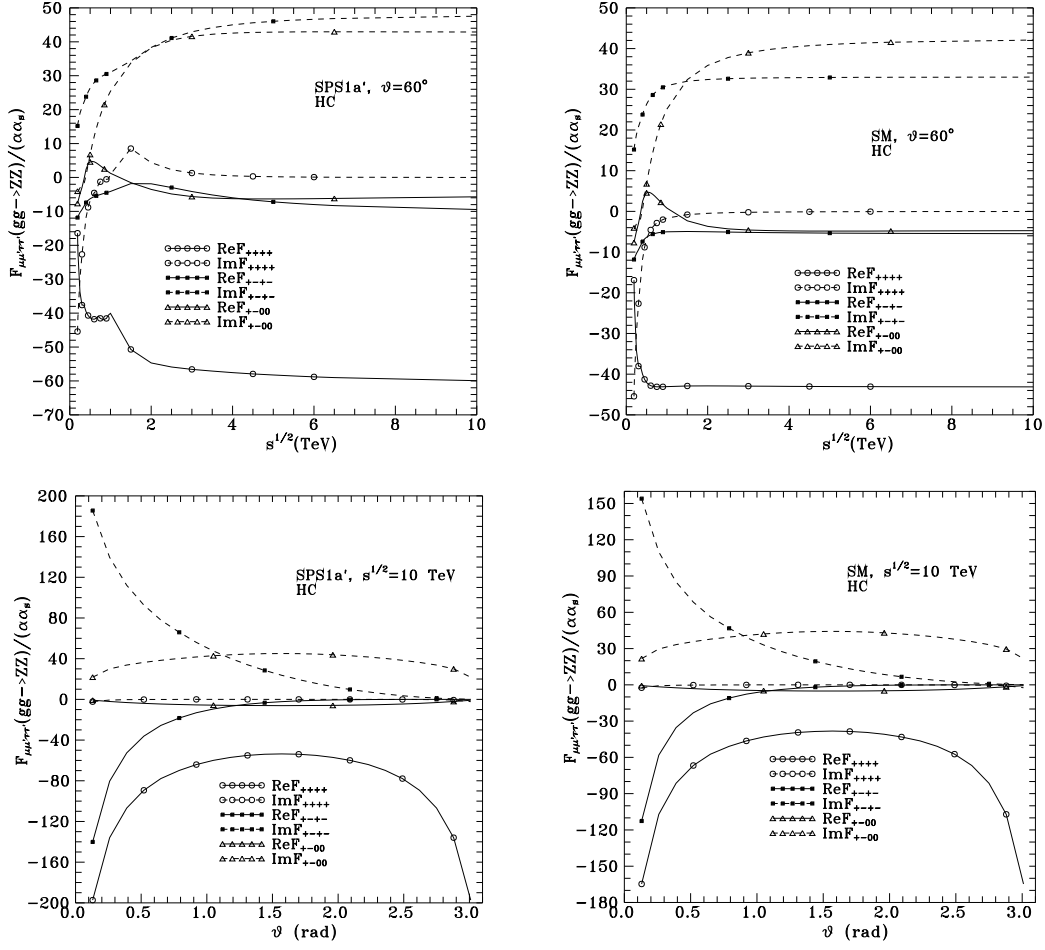


Figure 4: HC amplitudes for $gg \rightarrow ZZ$ in $SPS1a'$ and SM, as in Fig.2.

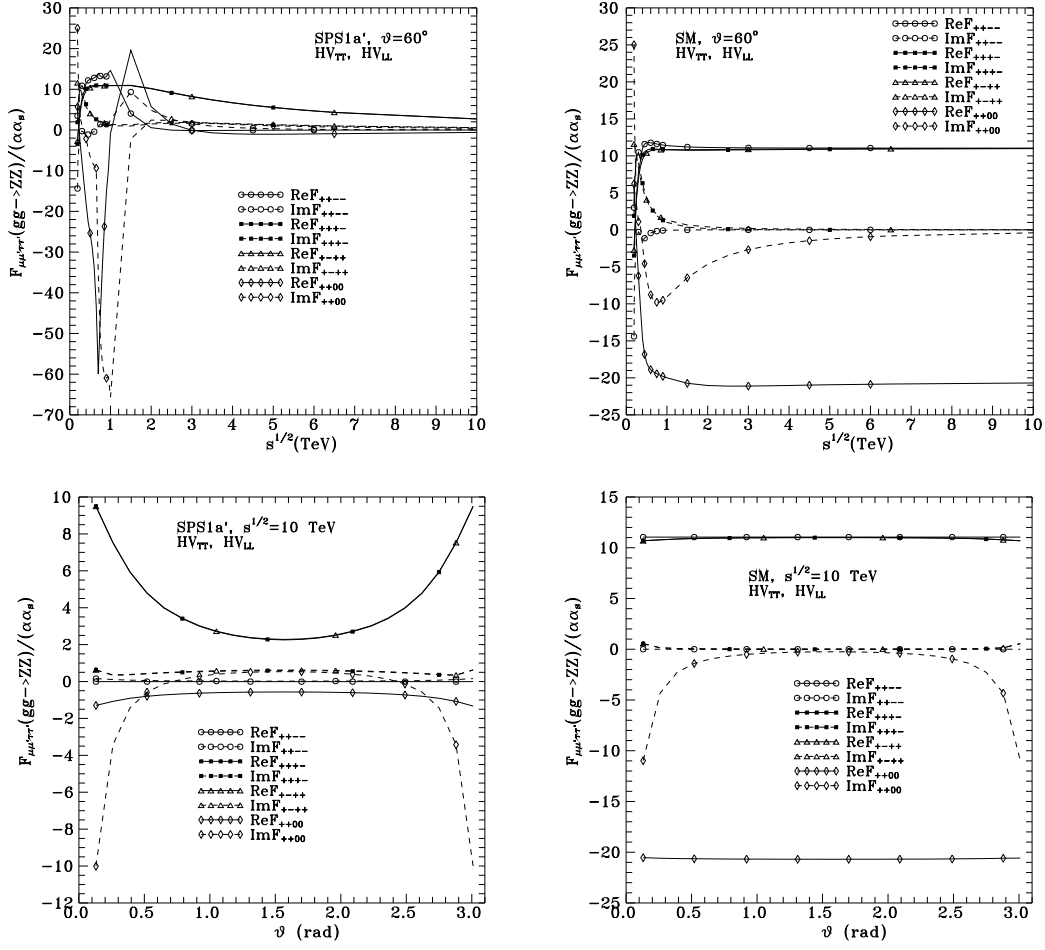


Figure 5: HV_{TT} and HV_{LL} amplitudes for $gg \rightarrow ZZ$ in $SPS1a'$ and SM, as in Fig.2.

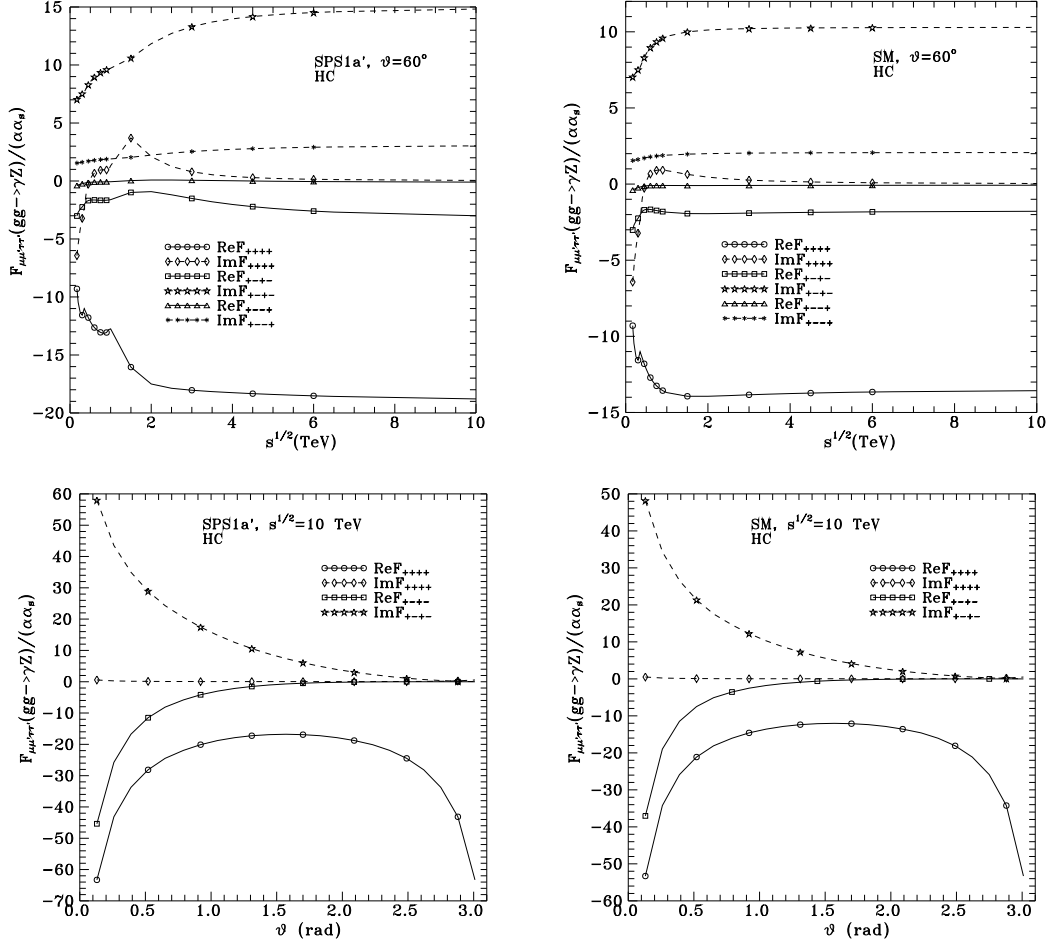


Figure 6: HC amplitudes for $gg \rightarrow \gamma Z$ in $SPS1a'$ and SM, as in Fig.2.

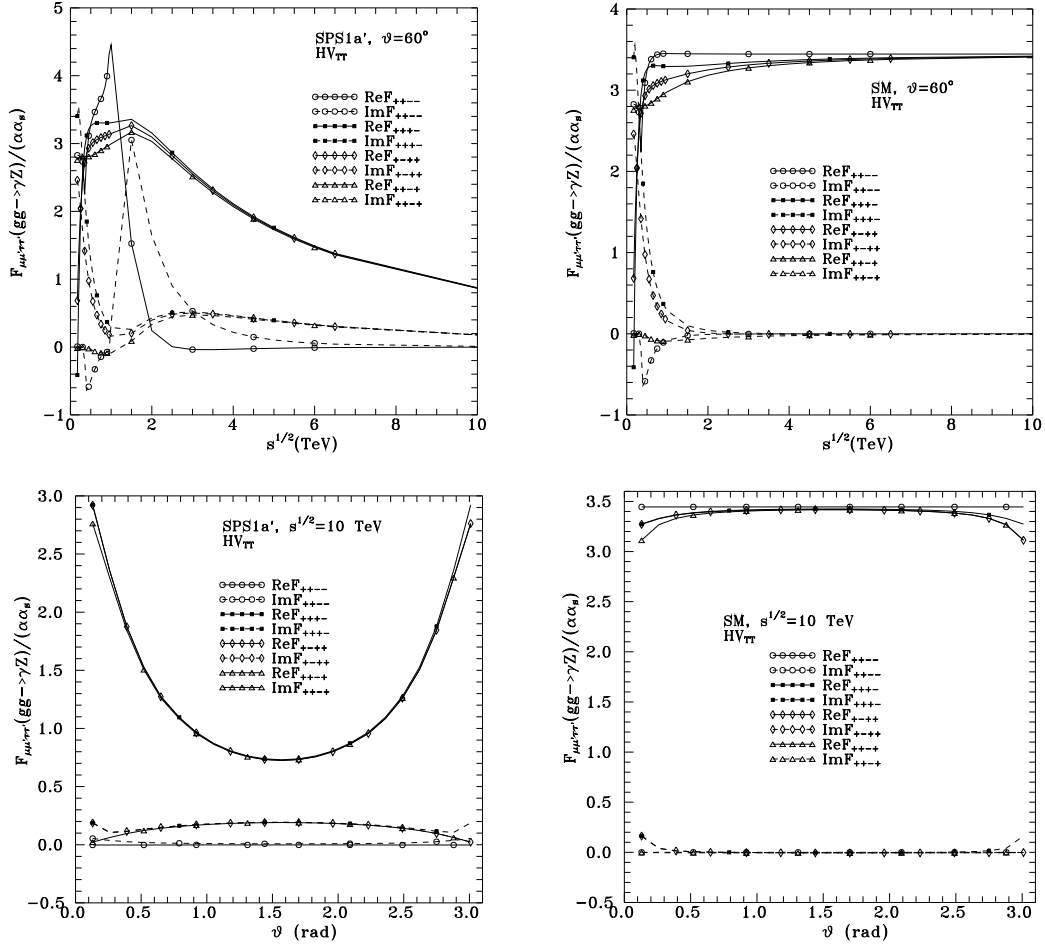


Figure 7: HV_{TT} -amplitudes for $gg \rightarrow \gamma Z$ in $SPS1a'$ and SM, as in Fig. 2.

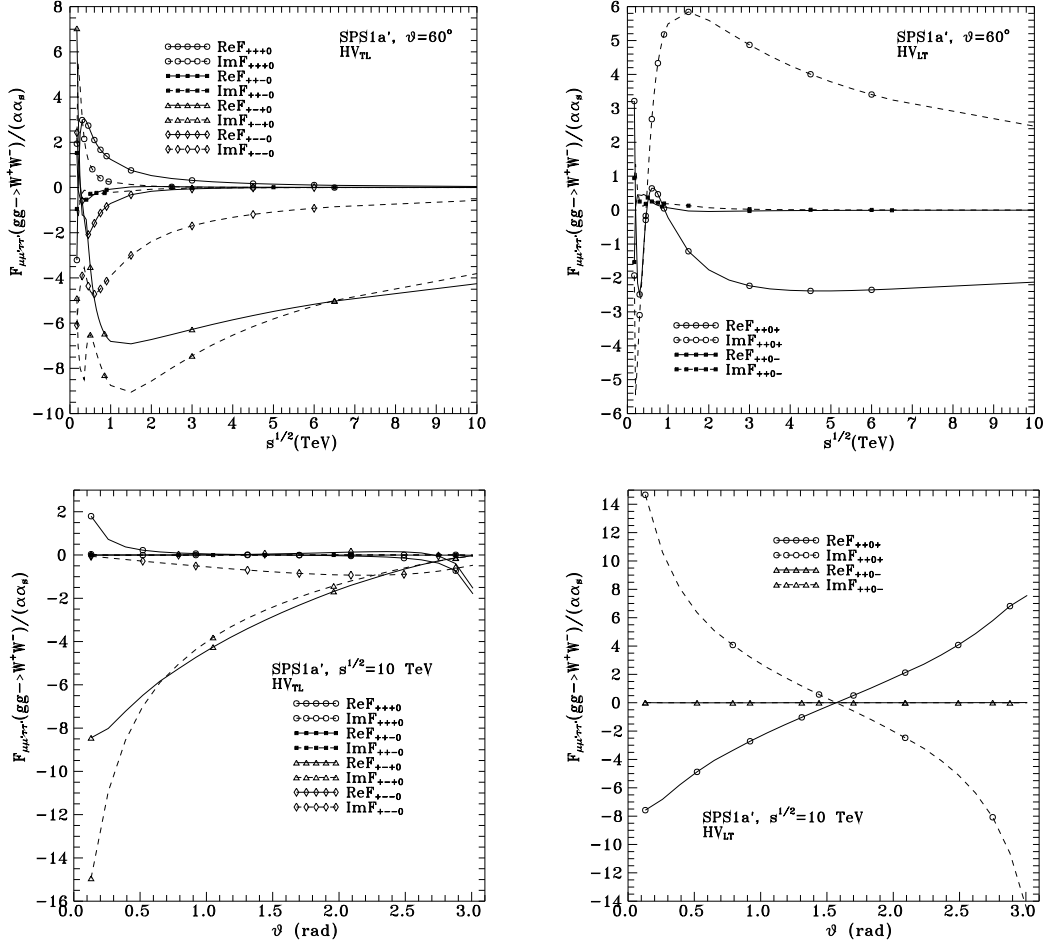


Figure 8: HV_{TL} (left panels) and HV_{LT} (right panels) amplitudes for $gg \rightarrow W^+W^-$ in $SPS1a'$; $\tau\tau' = 0$. Upper panels give the energy distributions at $\theta = 60^\circ$, while the lower panels give the angular distribution at $\sqrt{s} = 10$ TeV.

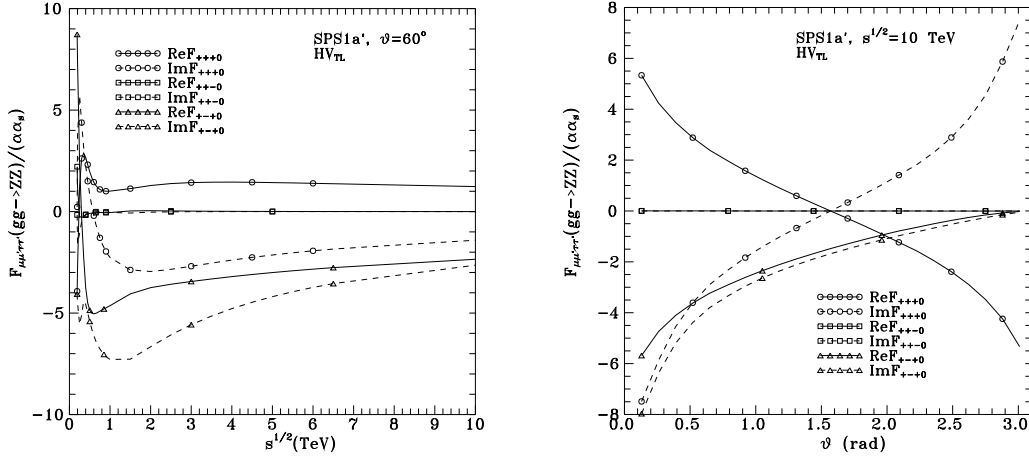


Figure 9: HV_{TL} amplitudes for $gg \rightarrow ZZ$ in $SPS1a'$. Left panel gives the energy distribution at $\theta = 60^\circ$, while the right panel gives the angular distribution at 10TeV.

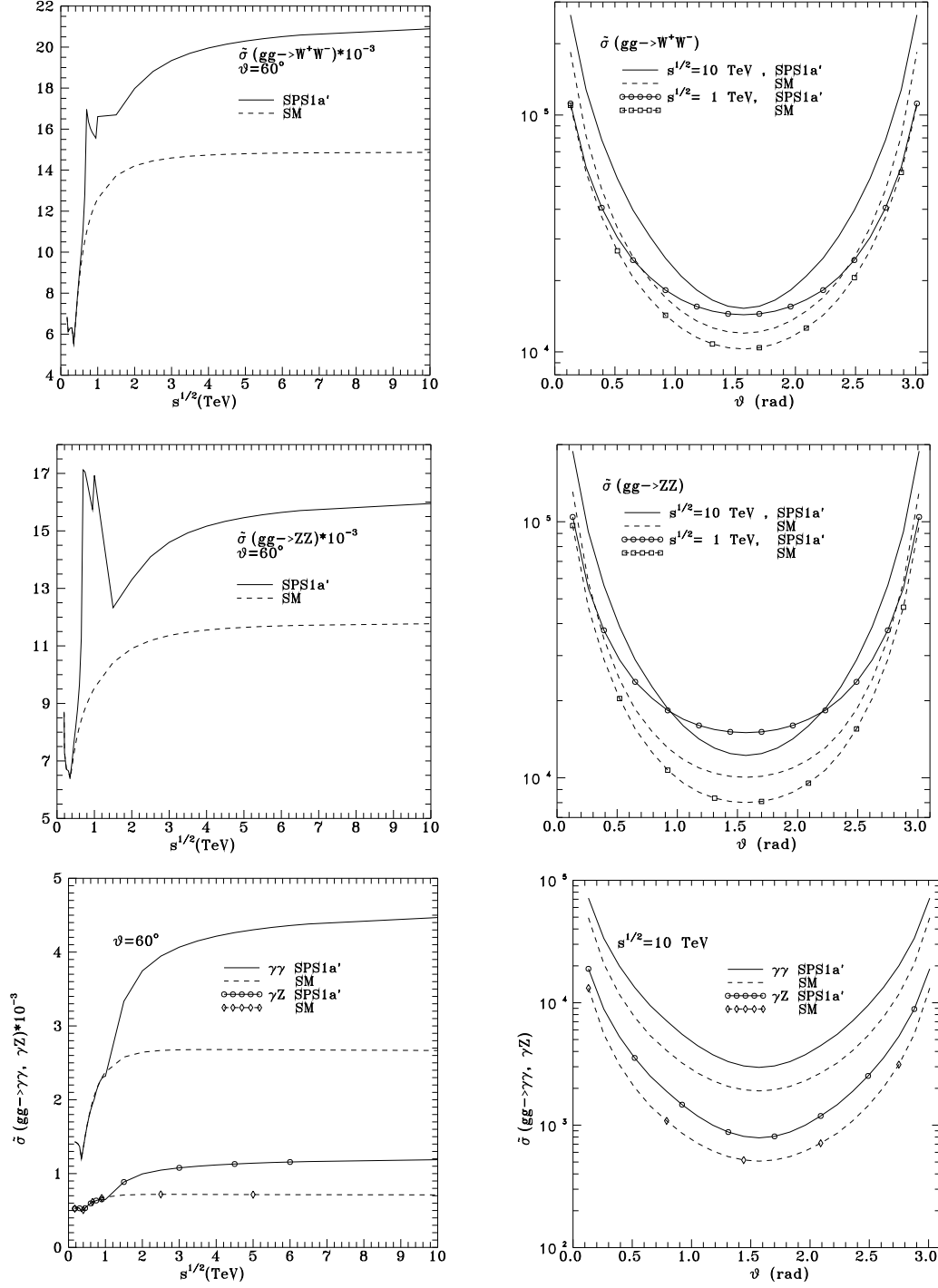


Figure 10: Dimensionless unpolarized differential cross sections for $\tilde{\sigma}(gg \rightarrow W^+W^-, ZZ, \gamma\gamma, \gamma Z)$ defined in (29), for $SPS1a'$ and SM. Left panels give the energy distributions, while right panels the angular ones.

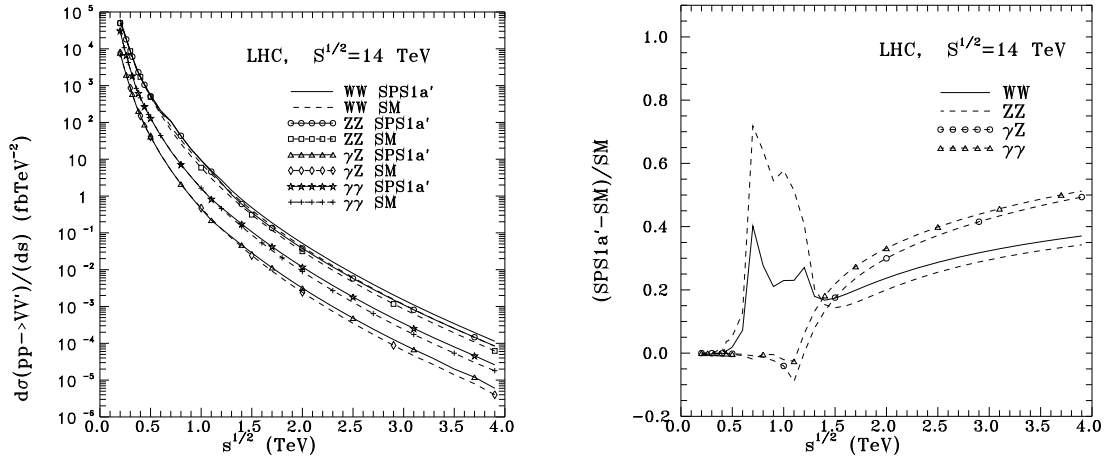


Figure 11: Left panel: The gluon fusion contribution to the LHC cross section as a function of the subprocess energy-squared s , for W^+W^- , ZZ , γZ and $\gamma\gamma$ production in $SPS1a'$ of MSSM and in SM. Right panel: The $SPS1a'$ result is compared to the SM one, for all these processes.